UDC 616.31-006.6:620.3:577.118 doi: https://doi.org/10.15407/ubj98.02.085

MOLECULAR EVALUATION OF BIOSYNTHESIZED SELENIUM NANOPARTICLES AND THEIR EFFECT ON ORAL SQUAMOUS CELL CARCINOMA

R. T. AL-MUSWIE[1], M. N. ABDULSAYED[2], D. A. ALGHEZI[3]✉, B. A. GHYADH[4], A. J. ALFAHDAWI[5]

[1]*Basic Science Department, College of Dentistry, University of Thi-Qar, Thi-Qar, Iraq;*
[2]*Otolaryngology-Head and Neck Department, College of Medicine, University of Thi-Qar, Thi-Qar, Iraq;*
[3]*Microbiology Department, College of Medicine, University of Thi-Qar, Thi-Qar, Iraq;*
[4]*Biology Department, College of Science, University of Thi-Qar, Thi-Qar, Iraq;*
[5]*Department of Pathological Analysis, College of Applied Sciences, University of Fallujah, Al-Anbar, Iraq;*
✉*e-mail: Dhafer.a.f.alghezi@bath.edu*

Received: 25 October 2025; **Revised:** 12 December 2025; **Accepted:** 03 April 2026

Cancer remains a predominant cause of mortality globally, and the suboptimal effectiveness of existing therapeutic modalities has catalyzed the exploration of novel treatment approaches. Nanomaterials, specifically selenium nanoparticles (SeNPs), have exhibited encouraging anticancer activity. This investigation aimed to evaluate the human oral squamous cell carcinoma (OSCC) cells viability and expression of proliferation and apoptosis molecular markers under treatment with SeNPs. Selenium nanoparticles were synthesized with the use of Lactobacillus plantarum cultured in a medium containing selenium dioxide. The methods of energy-dispersive X-ray, scanning electron and atomic force microscopy were used to determine the SeNPs composition and three-dimensional images. MTT viability assay and qRT-PCR analysis of cyclin D1 and Bax gene expression were applied. OSCC cells were treated with SeNPs in a range of 25–200 μg/ml for 24 h. It was demonstrated that SeNPs induced a dose-dependent inhibition of cell viability with IC_{50} value of 97 μg/ml. At lower concentrations (25–50 μg/ml) SeNPs transiently suppressed Bax and elevated Cyclin D1 expression, indicating the adaptive proliferative response. At higher concentrations (100–200 μg/ml), SeNPs induced apoptotic pathways and G1-phase cell cycle arrest, significantly upregulating Bax and downregulating Cyclin D1 expression. These findings underscore the Selenium nanoparticles potential as nanotherapeutic agents for OSCC treatment.

K e y w o r d s: selenium nanoparticles, oral squamous cell carcinoma, cyclin D, Bax.

Oral squamous cell carcinoma (OSCC), the predominant histopathological variant of oral malignancies, may arise in multiple intraoral sites, including the tongue, gingiva, palate, buccal mucosa, floor of the mouth, and lips. It is characterized by a notably high mortality rate despite advances in diagnostic and therapeutic modalities [1]. According to Radhika et al., OSCC accounts about 90% of oral cancer cases and ranks as the sixth most frequent malignancy globally [2]. The prognosis for OSCC remains poor, largely due to its frequent diagnosis at advanced stages and the presence of metastatic spread [3].

Nanoparticles (NPs) are ultra-fine particles measuring just 1–100 nanometers in diameter. They possess an exceptionally high surface-to-volume ratio and are subject to quantum confinement effects, which give rise to remarkable physical, chemical, optical, electrical, magnetic, and biological characteristics that markedly differ from those of the same materials in bulk form [4]. NPs have attracted considerable attention across various fields due to their potential applications in sectors, including medicine, electronics, energy production, and environmental remediation [5]. Due to their diminutive size, nanoparticles possess a markedly high surface-to-volume

ratio, which substantially augments their functional capabilities, chemical reactivity, and surface area available for molecular and interfacial interactions [6, 7]. The size, shape, and composition of NPs can be varied by a variety of synthesis techniques, including chemical, physical, and biological procedures [8]. The special qualities of NPs, however, call for careful evaluation of their possible effects on the environment and human health, which calls for in-depth research on their synthesis, characterization, and safe handling [9].

A trace element called selenium (Se) is essential to living things. The anti-cancer, antioxidant, anti-inflammatory, and antibacterial properties of red elemental selenium (Seo), often referred to as selenium nanoparticle (SeNP), have garnered significant interest among the various forms of Se [10]. Additionally, when compared to other selenium-containing substances, nanosized Se exhibits reduced toxicity, enhanced bioavailability, and lower production costs compared to its bulk counterparts [10].

SeNPs can be synthesized via a range of methodologies, encompassing physical, chemical, and biological methods. Among these, chemical synthesis represents the most common and rapid method used. Additionally, biological synthesis utilizing microorganisms and plant extracts has emerged as a sustainable and eco-friendly alternative [11]. According to published reports, oral administration of SeNPs in mice with metastatic breast cancer led to enhanced immune responses and a significant reduction in liver metastases [12, 13].

Selenium supplements have been employed as standalone anticancer agents owing to their well-documented antitumor properties [14]. Over the past ten years, SeNPs have been widely used as dietary supplements and potent antioxidants, due to their low risk compared to selenium alone. They have also been employed extensively in medical diagnosis [15]. Specifically, they have been sporadically informed to demonstrate antitumor activity against a broad spectrum of malignancies, including breast cancer, lung carcinoma, and gliomas, highlighting their potential as novel therapeutic agents in oncology [14, 15].

SeNPs have been shown to exert minimal effects on healthy cells while playing a critical role in suppressing lung cancer cells [16]. Similarly, studies on cervical carcinoma [17], hepatocarcinoma [18], and colorectal cancer [19] have demonstrated that SeNPs possess strong cytotoxic effects on tumor cells, with limited toxicity to normal cells. Thus, preparations were established to investigate the molecular processes of SeNPs and test for their inhibitory effects on additional cancer cells. SeNPs have been shown in preliminary investigations to be significantly active on a number of cancer cell lines, with their activity on SCC cells being stronger than that of other cancer cells. This suggests that SeNPs may be most useful in SCC and that they promote apoptosis and induce cell cycle arrest in a variety of SCC cell lines and freshly isolated tumor cells. Molecular biology studies indicate that SeNP-induced apoptosis is partly mediated through the upregulation of Bax and the downregulation of cyclin D expression. To investigate the effect of SNPs on cancer cell toxicity and cancer-related regulatory genes, Bax, a pro-apoptotic protein, and cyclin D1, an anti-apoptotic protein, were examined.

Materials and Methods

Cell line. The Iran Center of Cancer and Medical Genetics Research (ICCMGR) provides the human squamous carcinoma cell line SCC152. It was cultivated in Dulbecco's Modified Eagle's Medium (DMEM) supplemented with 10% fetal bovine serum and a 1% penicillin-streptomycin combination (Lonza, Verviers, Belgium). At 37°C, SCC152 cultures were incubated in a standard humidified environment with 95% air and 5% CO_2.

Selenium nanoparticles' preparation. Biogenic monovalent selenium nanoparticles were synthesized using *Lactobacillus plantarum* [20]. The procedure involved mixing 1 ml of a 254 mM selenium dioxide solution with a ml of *Lactobacillus plantarum* culture (OD_{600} = 1) and 100 ml of fresh MRS medium, then incubating the blend for 72 h at 37°C. After incubation, the red intracellular selenium was harvested from the bacterial pellets through sonication and rapid freezing in liquid nitrogen. The resulting Se^+ nanoparticles were further purified via a two-phase extraction using n-octanol and water [21]. The final nanoparticle suspension was kept at 4°C for further needs.

Atomic force microscopy (AFM). Energy-dispersive X-ray spectroscopy (EDS) in conjunction with scanning electron microscopy (SEM) was used to determine the basic composition of the purified nanoparticles. SeNPs in powder form were gently adhered to SEM stubs with adhesive tape covered with a uniform layer of carbon (LEICA EM ACE200, Wetzlar, Germany). The prepared stubs

were then placed into the SEM-EDS instrument (Zeiss EVOMA10, Oberkochen, Germany, equipped with an Oxford Instruments X-act EDX system) for analysis. Imaging was performed at an accelerating voltage of 20 kV with a magnification of 1500×.

Energy-dispersive X-ray spectroscopy (EDS). The purified NPs' elemental composition was determined using SEM and EDS. SeNPs (powder) were carefully mounted on SEM stubs using adhesive tape that was evenly coated with carbon (LEICA EM ACE200, Wetzlar, Germany). The tape was then put in an SEM-EDS sample chamber (Zeiss EVOMA10, Oberkochen, Germany; Oxford Instruments X-act EDX system). The scans were conducted at a voltage of 20 kV and a magnification of 1500×.

Fourier-transformed infrared spectroscopy FTIR spectroscopy. FTIR spectroscopy was conducted to recognize the functional groups involved in the biosynthesis of SeNPs. The spectra of the dried samples were acquired using an ALPHA FT-IR-ATR Bruker Spectrometer across a wavenumber range of 400–4000 cm^{-1}, with a resolution of 1 cm^{-1} and a total of 100 scans. Each spectrum underwent baseline correction via the instrument's "automatic baseline correct" feature, followed by smoothing using the standard "automatic smooth" function, which applies a Savitzky–Golay algorithm with a 95-point moving second-degree polynomial filter.

MTT assay. SeNPs were tested for their anticancer activity against a variety of tumor cell lines using the MTT assay (3-(4,5-dimethylthiazol-2-yl)-2,5-diphenyltetrazolium bromide). Initially, cells were first counted and seeded at a density of 10,000 cells per well into 96-well plates, where they were left to adhere for a full day. After that, cells were exposed to preset SeNP concentrations for a further twenty-four hours. To promote formazan production, MTT reagent was applied after treatment and incubated for three hours. Following the addition of dimethyl sulfoxide (DMSO) to dissolve the formazan crystals, the plates were allowed to stand for fifteen minutes. After that, utilizing a DYNEX ELISA microplate reader (USA), the absorbance at 570 nm was measured. An optical density (OD) to cell count calibration curve was created. The appropriate OD values were used to interpolate the cell numbers after treatment. The following formula was used to measure the inhibitory impact of SeNPs:

Inhibition rate = (cell number (control) − cell number (SeNP treatment))/cell number(control)× 100%.

Reverse transcription-quantitative polymerase chain reaction (RT-qPCR) assay. Total cellular RNA was harvested utilizing TRIzol reagent (Invitrogen, Grand Island, NY, USA). After extraction, quantitative reverse transcription PCR (qRT-PCR) targeting mRNA was conducted with the Prime Script RT-PCR kit (Takara Bio Inc., Shiga, Japan) on a Bio-Rad IQ5 real-time PCR instrument (Hercules, CA, USA).

To denature the secondary structures of RNA, the material was first incubated for five minutes at 65°C. Next, it was heated to 37°C for 15 min to allow for the synthesis of first-strand cDNA. Finally, it was heated to 98°C for five minutes to inactivate the reverse transcriptase enzyme. For the PCR amplification that followed, a preliminary denaturation was performed for 30 sec at 95°C. 40 amplification cycles were then performed, with primer annealing at 60°C for five seconds, extension at 72°C for thirty seconds, and denaturation at 95°C for five seconds in each cycle.

The $2^{-\Delta\Delta CT}$ method [22] was used to examine the data by a comparative threshold (Ct), and the mean fold inductions of the samples were compared with the untreated samples. Table 1 provides a description of the primer sequences for each target and GAPDH.

Statistical analysis. GraphPad Prism version 8.4.3 (GraphPad Software, San Diego, CA, USA) was used to examine the data described as group means ± SEM. The data were investigated via two-way ANOVA with multiple Tukey's tests. Differences were considered significant when the *P*-value was < 0.05.

Results and Discussion

In 2012, lip and oral cavity cancers accounted for approximately 2.1% of all malignancies globally, with males representing two-thirds of the cases.

Table 1. Shows the primers' sequences for qPCR

Target gene	Primer sequences
Cyclin D1	F: TGAACTACCTGGACCGCT R: CTCTGGCATTTTGGAG
GAPDH	F: TCAAGGAGGAGTCTGAGGGA R: TCCAGCCTTGGCATCG
BAX	F: GGTTGTCGCCCTTTTCTA R: GGCGTACAGGGATAGC

The highest incidence rates for both sexes were observed in Melanesia. Additionally, elevated rates among men were noted in Central and Eastern Europe (9.1 per 100,000) and South-Central Asia (9.9 per 100,000). Worldwide, these cancers resulted in an estimated 145,000 deaths, with 77% of fatalities occurring in less developed regions [22].

OSCC starts with oral epithelial dysplasia, in which the epithelial cells exhibit atypia and dysplastic alterations in the tissue itself [23, 24]. The basement membrane is then disturbed, allowing cancer cells to enter the surrounding stroma and cause reactive alterations. The cancer cells' biological behavior is governed by both their genetic composition and the tumor microenvironment, which allows the tumor cells to thrive due to the stromal and epithelial component' faulty responses [25, 26].

Morphological and Structural Characterization of SeNPs

Atomic force microscopy (AFM) was employed to generate three-dimensional topographical images of the synthesized SeNPs. As illustrated in Fig. 1, the SeNPs displayed predominantly spherical morphology with a polydisperse distribution. The 3D topographical maps revealed smooth surface features, and the average vertical height was approximately 15 nm, supporting observations from transmission electron microscopy. The spherical, uniform morphology is indicative of successful capping and stabilization, which is crucial for biological interactions and cellular uptake.

Fourier-transform infrared spectroscopy (FTIR) analysis further confirmed the biochemical composition of Lactiplantibacillus plantarum-mediated SeNPs. The FTIR spectrum (Fig. 2) exhibited a broad peak at 3441.38 cm^{-1}, corresponding to N–H and O–H stretching, indicative of alcohols, phenols, amides, and amines. Peaks at 2924.62 and 2853.56 cm^{-1} were attributed to C–H stretching of aliphatic hydrocarbons, suggesting the involvement of alkyl chains in capping. The presence of a peak at 2177.31 cm^{-1} indicated C≡C stretching (alkyne groups), and the band at 1642.88 cm^{-1} corresponded to C=C stretching in conjugated alkenes. Notably, a distinct peak at 725.95 cm^{-1} suggested aromatic C–H bending. These chemical features collectively support the hypothesis that proteins and phenolic compounds mediate SeNP stabilization, as reported in other studies [27, 28].

Energy-dispersive X-ray spectroscopy (EDX) confirmed the elemental composition of the nanoparticles (Fig. 3). The selenium content was 20.24 wt%, while other elements included N (20.15%), O (10.48%), C (5.1%), S (0.72%), Si (0.36%), and K (0.19%). These findings substantiate the organic–inorganic hybrid nature of the SeNPs, with surface-bound biomolecules likely contributing to biocompatibility and stability in physiological environments [28].

In vitro antitumor activity of SeNPs. The antineoplastic potential of SeNPs was evaluated against OSCC cell lines. As presented in Fig. 4, SeNPs induced a dose-dependent inhibition of cell proliferation. The most significant cytotoxic effect was observed at 200 μg/ml, with a statistically significant reduction in cell viability compared to control groups ($P \leq 0.001$). These findings align with previous studies indicating that the physicochemical attributes of SeNPs – such as particle size, surface charge, and composition–profoundly influence cellular uptake and bioactivity [29, 30].

The IC_{50} value for SeNPs was determined to be 97 μg/ml, demonstrating moderate cytotoxicity and aligning with selenium's known anticancer profile. Importantly, selenium nanoparticles are known to exhibit preferential toxicity toward malignant cells while sparing normal tissue, making them suitable candidates for chemotherapeutic development [31].

Apoptosis and gene expression modulation. To clarify the molecular pathways that contribute to SeNP-induced cytotoxicity, quantitative reverse transcription polymerase chain reaction (qRT-PCR) was utilized to evaluate the expression levels of Bax, a pro-apoptotic biomarker, and Cyclin D1 (CCND1), a key regulator of the G1 phase of the cell cycle, in oral squamous cell carcinoma (OSCC) cell lines. The investigation assessed the impact of differing concentrations of selenium nanoparticles (SeNPs) on the expression of these genes.

The findings demonstrated a dose-dependent, reciprocal modulation of both genes. At lower concentrations (25 and 50 μg/ml), SeNPs significantly reduced Bax expression while simultaneously elevating CCND1 levels. In contrast, at higher concentrations (100 and 200 μg/ml), there was an upregulation of Bax and a downregulation of CCND1, suggesting a transition from proliferative to apoptotic mechanisms ($P < 0.05$) [32, 33].

This inverse relationship suggests a biphasic effect, consistent with previous study [34]. At sub-toxic levels, nanoparticles may induce mild stress that transiently activates cell cycle-associated genes like CCND1, facilitating temporary cell sur-

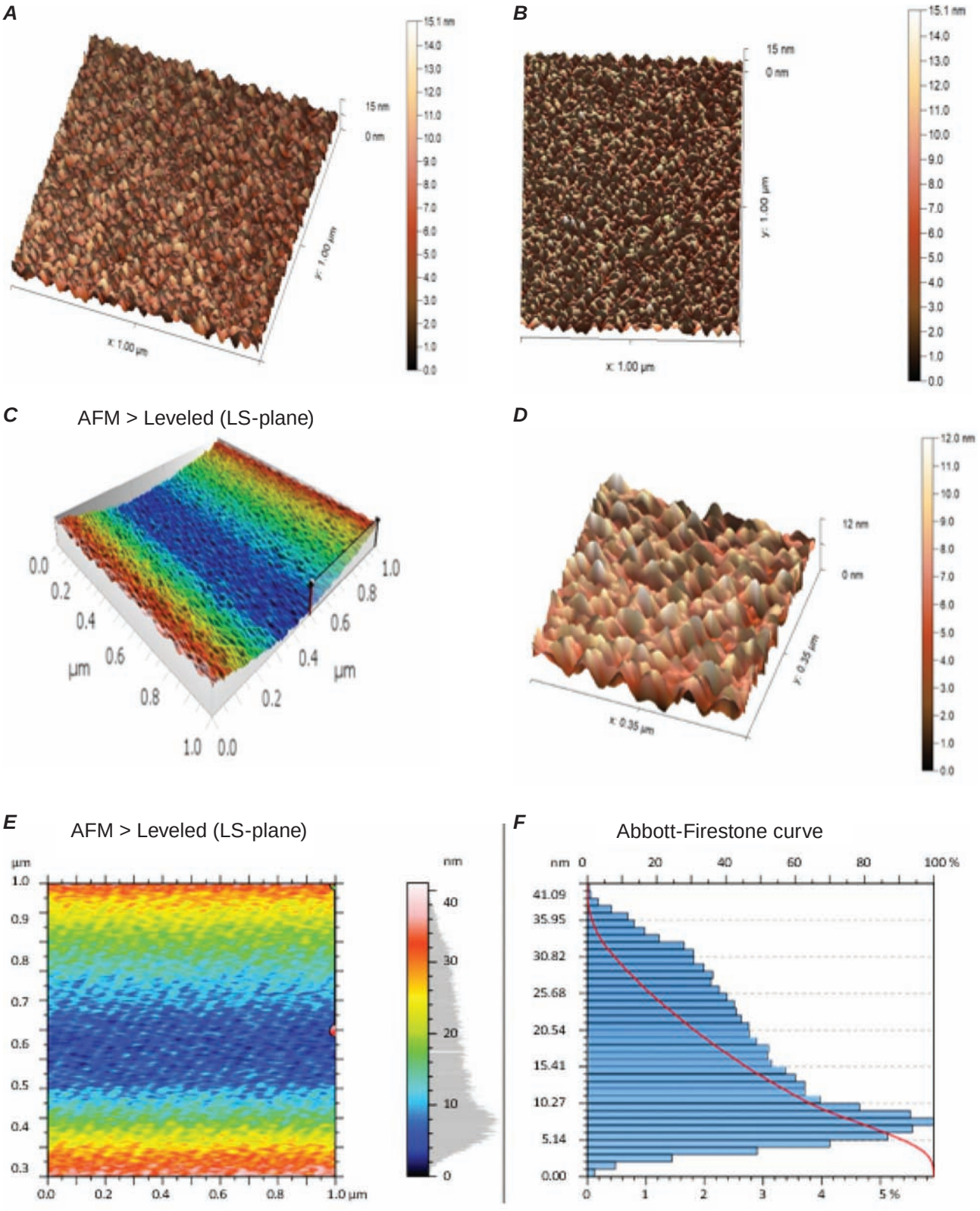

*Fig. 1. Tapping mode AFM topographical images of the SeNPs. (**A**) 3–D images, (**B**) Scan area of SeNPs in 2–D image, (**C**) histogram height profile, (**D**) 3–D images, (**E**) histogram height profile, (**F**) histogram height profile*

Spectrum name	Number of peaks
R	6

R Details:

Peaks number	X (cm^{-1})	Y (%T)
1	3441.38	28.59
2	2924.62	36.29
3	2853.56	37.59
4	2177.31	38.03
5	1642.88	36.82
6	725.95	58.73

R Spectra

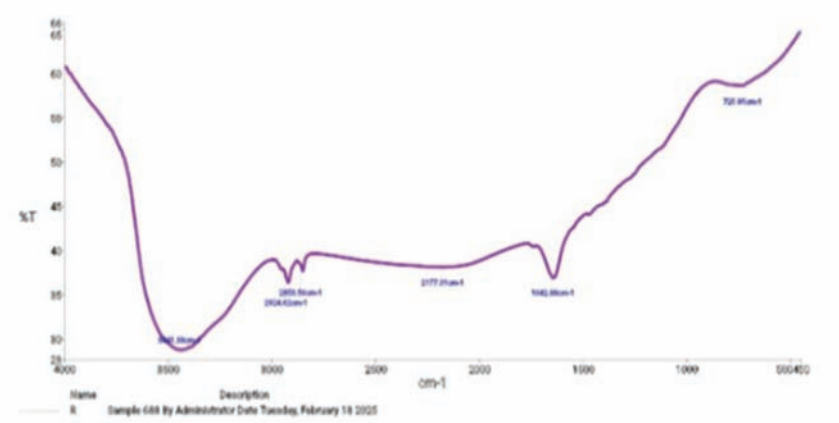

Fig. 2. Fourier-transform infrared spectroscopy demonstrates the structural features of SeNPs generated by Lactobacillus plantarum HM1

vival. However, surpassing a certain concentration threshold causes SeNPs to instigate oxidative stress, mitochondrial impairment, and apoptosis, leading to Bax activation and a decrease in cellular proliferation [27, 33].

Despite the low-dose profile (decreased Bax, increased CCND1) potentially indicating enhanced proliferation, it contradicts the observed reduction in OSCC cell viability at these concentrations. This apparent inconsistency likely stems from the fact that alterations in gene expression do not invariably correlate with functional consequences. The initial rise in CCND1 may signify a fleeting adaptive response to oxidative stress rather than actual proliferation [34].

Apoptosis may also transpire independently of Bax transcription, through the generation of reactive oxygen species (ROS) and the activation of caspases [35]. Therefore, the diminished viability observed at 25–50 μg/ml could be attributed to oxidative damage occurring prior to Bax upregulation. Furthermore, SeNPs exert effects in a time-dependent manner, wherein early adaptive gene expression precedes subsequent cytotoxic outcomes, including cell cycle arrest and apoptosis [36]. Taken together, these results underscore the intricate, dose- and time-dependent dynamics between proliferative and apoptotic signaling within SeNP-treated OSCC cells.

As shown in Fig. 5 and 6, SeNP exposure at 100 and 200 μg/ml significantly upregulated Bax expression and concurrently downregulated cyclin D1 ($P < 0.05$). The elevation of Bax mRNA supports the hypothesis that SeNPs activate intrinsic apoptotic pathways, potentially via mitochondrial destabilization and caspase cascade initiation [31, 37]. Cyclin D1 downregulation further suggests SeNP-induced cell cycle arrest at the G1 phase, impairing DNA replication and proliferation. Overexpression of cyclin

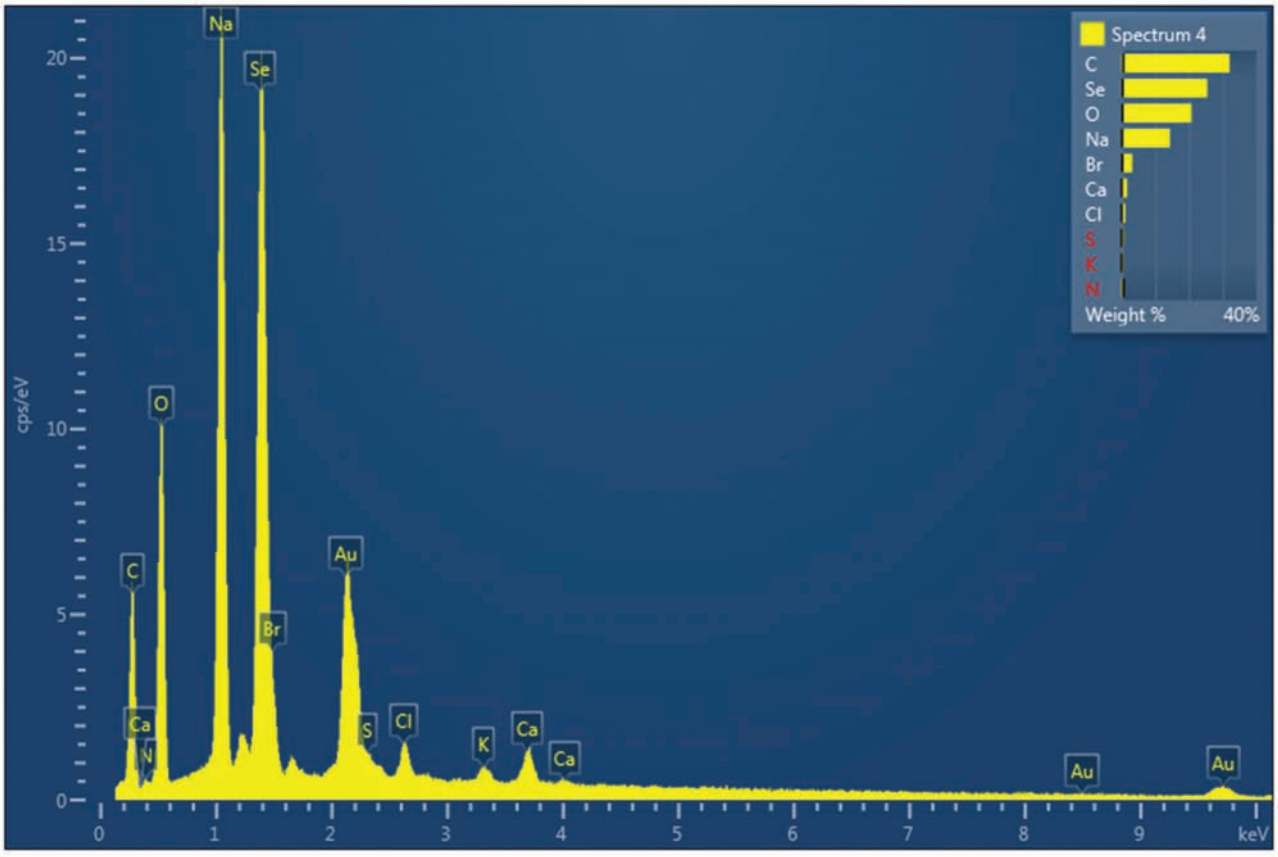

Fig. 3. Shows the structural properties of SeNPs, which are produced by Lactobacillus plantarum HM1, examined using energy-dispersive X-ray spectroscopy

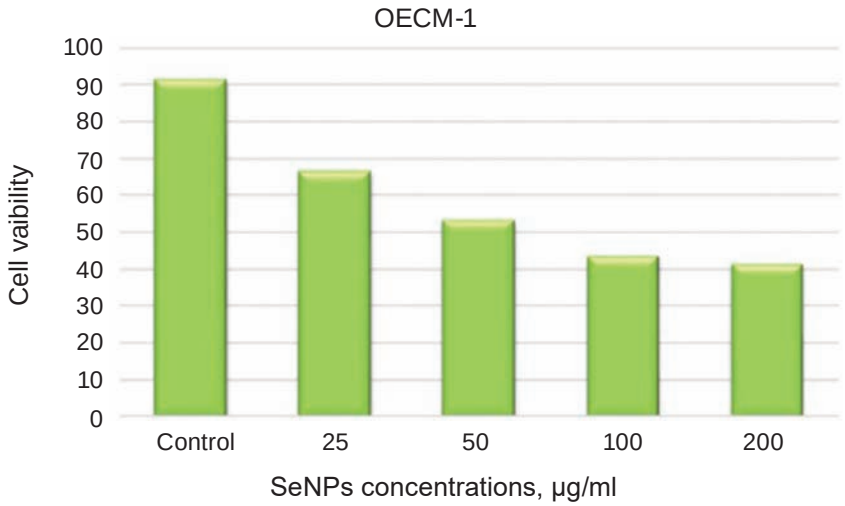

*Fig. 4. In vitro antitumor efficacy of SeNPs against OSCC cells. The percentage of inhibition of OSCC cell proliferation was dose-dependent, with SeNP concentrations ranging from 50 to 200 µg/ml, demonstrating robust anticancer activity as shown. X-axis represents SeNP concentrations (µg/ml); Y-axis represents relative cell viability. *P ≤ 0.001*

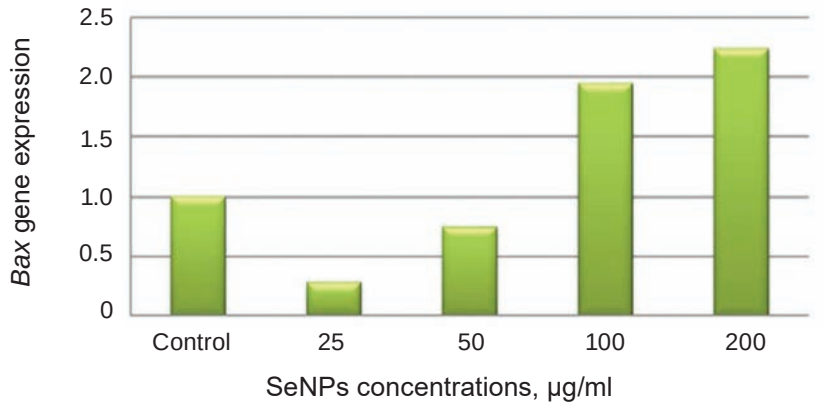

*Fig. 5. Expression of Bax in OSCC line in response to exposure to selenium nanoparticles, comparison with control. Bax mRNA levels were quantified by qRT-PCR and normalized to control. X-axis represents SeNP concentrations (μg/ml); Y-axis represents relative Bax expression. *P < 0.05*

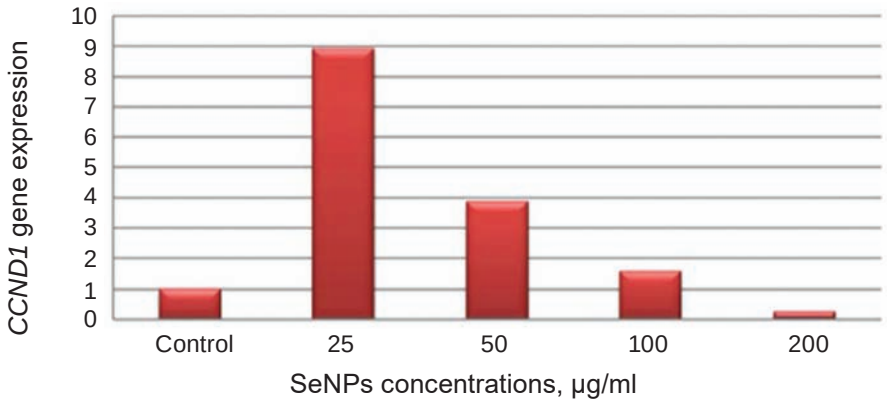

*Fig. 6. Cyclin D1 expression in OSCC line in response to exposure to selenium nanoparticles, comparison with control. Cyclin D1 mRNA levels were quantified by qRT-PCR and normalized to control. X-axis represents SeNP concentrations (μg/ml); Y-axis represents relative cyclin D1 expression. *P < 0.05*

D1 is a known driver of oncogenesis through uncontrolled cellular growth and genomic instability; thus, its inhibition is consistent with antiproliferative activity [38-40].

Mechanistic insights and comparative studies. The antitumor efficacy of SeNPs is thought to result from multiple converging pathways, including oxidative stress modulation, mitochondrial dysfunction, and ER stress-mediated apoptosis. SeNPs can induce caspase activation, ROS generation, and DNA damage responses [41, 42]. Notably, SeNPs also exhibit reduced toxicity compared to inorganic selenium forms, which enhances their translational potential [41].

Huang et al. [43] demonstrated that SeNPs promote autophagy in cancer cells, while Sonkusre and Cameotra [27] showed SeNP-induced necrosis through TNF elevation. Another study indicated that SeNPs inhibit DNA, RNA, and protein biosynthesis, suggesting potential modulation of non-coding RNA expression [44]. These findings underscore the multifactorial mechanisms through which SeNPs exert their cytotoxicity.

Molecular targets of SeNPs. Cyclin D1 is primarily expressed during the G1 phase of the cell cycle, playing a critical role in integrating mitogenic signals with the cell cycle machinery [38]. Its dysregulation leads to uncontrolled proliferation and genomic instability [38, 39]. In contrast, Bax, a pro-apoptotic gene, promotes apoptosis via mitochondrial pathway activation and is commonly upregulated following exposure to cytotoxic agents [45]. The present findings, showing increased Bax and reduced cyclin D1 expression, support the dual

anticancer role of SeNPs as inducers of apoptosis and inhibitors of cell proliferation.

Conclusion. This study shows that SeNPs have a strong cytotoxic impact on OSCC cells in a concentration-dependent manner. Treatment with higher doses of SeNPs significantly reduced cell viability and induced apoptosis, as evidenced by the downregulation of the anti-apoptotic gene cyclin D1 and the upregulation of the pro-apoptotic gene Bax. These molecular changes suggest that SeNPs trigger apoptotic pathways, contributing to their anticancer efficacy. Given their selective toxicity toward cancer cells and reduced harm to normal tissues, SeNPs represent a promising therapeutic approach for oral cancer. Further, in vivo investigations and mechanistic studies are warranted to validate their clinical potential and elucidate the detailed pathways involved in SeNP-induced tumor suppression.

Conflict of interest. The authors have completed the Unified Conflicts of Interest form at http://ukr-biochemjournal.org/wp-content/uploads/2018/12/coi_disclosure.pdf and declare no conflict of interest.

Funding. No funding was received for this study.

МОЛЕКУЛЯРНА ОЦІНКА БІОСИНТЕЗОВАНИХ НАНОЧАСТИНОК СЕЛЕНУ ТА ЇХ ВПЛИВ НА ПЛОСКОКЛІТИННУ КАРЦИНОМУ РОТОВОЇ ПОРОЖНИНИ

R. T. Al-Muswie[1], M. N. Abdulsayed[2], D. A. Alghezi[3]✉, B. A. Ghyadh[4], A. J. Alfahdawi[5]

[1]Basic Science Department, College of Dentistry, University of Thi-Qar, Thi-Qar, Iraq;
[2]Otolaryngology-Head and Neck Department, College of Medicine, University of Thi-Qar, Thi-Qar, Iraq;
[3]Microbiology Department, College of Medicine, University of Thi-Qar, Thi-Qar, Iraq;
[4]Biology Department, College of Science, University of Thi-Qar, Thi-Qar, Iraq;
[5]Department of Pathological Analysis, College of Applied Sciences, University of Fallujah, Al-Anbar, Iraq;
✉e-mail: Dhafer.a.f.alghezi@bath.edu

Рак залишається однією з провідних причин смертності у світі, а недостатня ефективність наявних терапевтичних підходів стимулює пошук нових методів лікування. Наноматеріали, зокрема наночастинки селену (SeNPs), демонструють перспективну протипухлинну активність. Метою цього дослідження було оцінити життєздатність клітин плоскоклітинної карциноми ротової порожнини людини (OSCC), а також експресію молекулярних маркерів проліферації та апоптозу під впливом SeNPs. Наночастинки селену синтезували з використанням *Lactobacillus plantarum*, культивованих у середовищі, що містило діоксид селену. Для визначення складу наночастинок SeNPs та отримання їхніх тривимірних зображень застосовували методи енергодисперсійної рентгенівської спектроскопії, сканувальної електронної мікроскопії та атомно-силової мікроскопії. Оцінку життєздатності клітин проводили за допомогою MTT-тесту, а аналіз експресії генів цикліну D1 і Bax - методом qRT-PCR. Клітини OSCC обробляли SeNPs у концентраціях 25–200 мкг/мл протягом 24 год. Показано, що SeNPs спричиняли дозозалежне пригнічення життєздатності клітин із значенням IC_{50} 97 мкг/мл. За нижчих концентрацій (25–50 мкг/мл), SeNPs тимчасово пригнічували експресію Bax та підвищували експресію цикліну D1, що свідчить про адаптивну проліферативну відповідь. За вищих концентрацій (100–200 мкг/мл), SeNPs індукували апоптоз та зупинку клітинного циклу у фазі G1, що супроводжувалося значним підвищенням експресії Bax і зниженням експресії цикліну D1. Отримані результати підкреслюють потенціал наночастинок селену як нанотерапевтичних засобів для лікування OSCC.

Ключові слова: наночастинки селену, плоскоклітинна карцинома порожнини рота, циклін D1, Bax.

References

1. Tan Y, Wang Z, Xu M, Li B, Huang Z, Qin S, Nice EC, Tang J, Huang C. Oral squamous cell carcinomas: state of the field and emerging directions. *Int J Oral Sci*. 2023; 15(1): 44.
2. Radhika T, Jeddy N, Nithya S, Muthumeenakshi RM. Salivary biomarkers in oral squamous cell carcinoma - An insight. *J Oral Biol Craniofac Res*. 2016; 6(Suppl 1): S51-S54.
3. Forastiere A, Koch W, Trotti A, Sidransky D. Head and neck cancer. *N Engl J Med*. 2001; 345(26): 1890-1900.

4. Khan S, Hossain MK. Classification and Properties of Nanoparticles. In: Nanoparticle-Based Polymer Composites. 2022. p. 15-54.
5. Varadavenkatesan T, Nagendran V, Vinayagam R, Goveas LC, Selvaraj R. Effective degradation of dyes using silver nanoparticles synthesized from *Thunbergia grandiflora* leaf extract. *Bioresour Technol Rep.* 2024; 27: 101914.
6. Ahmad Z, Shah SA, Khattak I, Ullah H, Khan AA, Shah RA, et al. Melia Azedarach impregnated Co and Ni zero-valent metal nanoparticles for organic pollutants degradation: validation of experiments through statistical analysis. *J Mater Sci: Mater Electron*. 2020; 31: 16938-16950.
7. Selvaraj R, Nagendran V, Varadavenkatesan T, Goveas LC, Vinayagam R. Stable silver nanoparticles synthesis using Tabebuia aurea leaf extract for efficient water treatment: A sustainable approach to environmental remediation. *Chem Eng Res Des.* 2024; 208: 456-463.
8. Rukhsar M, Ahmad Z, Rauf A, Zeb H, Ur-Rehman M, Hemeg HA. An Overview of Iron Oxide (Fe_3O_4) Nanoparticles: From Synthetic Strategies, Characterization to Antibacterial and Anticancer Applications. *Crystals.* 2022; 12(12): 1809.
9. Rauf A, Rashid U, Atta A, Khan I, Shah ZA, Mobeen B, Javed A, Alomar TS, Almasoud N, Naz S, Ahmad Z, Ribaudo G. Antiproliferative Activity of Lignans from Olea ferruginea: *In Vitro* Evidence Supported by Docking Studies. *Front Biosci (Landmark Ed).* 2023; 28(9): 216.
10. Forootanfar H, Adeli-Sardou M, Nikkhoo M, Mehrabani M, Amir-Heidari B, Shahverdi AR, Shakibaie M. Antioxidant and cytotoxic effect of biologically synthesized selenium nanoparticles in comparison to selenium dioxide. *J Trace Elem Med Biol*. 2014; 28(1): 75-79.
11. Skalickova S, Milosavljevic V, Cihalova K, Horky P, Richtera L, Adam V. Selenium nanoparticles as a nutritional supplement. *Nutrition*. 2017; 33: 83-90.
12. Faghfuri E, Yazdi MH, Mahdavi M, Sepehri-zadeh Z, Faramarzi MA, Mavandadnejad F, Shahverdi AR. Dose-response relationship study of selenium nanoparticles as an immunostimulatory agent in cancer-bearing mice. *Arch Med Res.* 2015; 46(1): 31-37.
13. Yazdi MH, Mahdavi M, Varastehmoradi B, Faramarzi MA, Shahverdi AR. The immuno-stimulatory effect of biogenic selenium nanoparticles on the 4T1 breast cancer model: an *in vivo* study. *Biol Trace Elem Res.* 2012; 149(1): 22-28.
14. Tugarova AV, Mamchenkova PV, Dyatlova YA, Kamnev AA. FTIR and Raman spectroscopic studies of selenium nanoparticles synthesised by the bacterium *Azospirillum thiophilum*. *Spectrochim Acta A Mol Biomol Spectrosc*. 2018; 192: 458-463.
15. Winkler HC, Suter M, Naegeli H. Critical review of the safety assessment of nano-structured silica additives in food. *J Nanobiotechnology*. 2016; 14(1): 44.
16. Liu S, Wei W, Wang J, Chen T. Theranostic applications of selenium nanomedicines against lung cancer. *J Nanobiotechnology*. 2023; 21(1): 96.
17. Zhou Y, Xu M, Liu Y, Bai Y, Deng Y, Liu J, Chen L. Green synthesis of Se/Ru alloy nanoparticles using gallic acid and evaluation of theiranti-invasive effects in HeLa cells. *Colloids Surf B Biointerfaces.* 2016; 144: 118-124.
18. Wang X, Sun K, Tan Y, Wu S, Zhang J. Efficacy and safety of selenium nanoparticles administered intraperitoneally for the prevention of growth of cancer cells in the peritoneal cavity. *Free Radic Biol Med*. 2014; 72: 1-10.
19. Gao F, Yuan Q, Gao L, Cai P, Zhu H, Liu R, Wang Y, Wei Y, Huang G, Liang J, Gao X. Cytotoxicity and therapeutic effect of irinotecan combined with selenium nanoparticles. *Biomaterials.* 2014; 35(31): 8854-8866.
20. Zare H, Sanaei M, Yazdi MH, Shahverdi AR. Selenium nanoparticle-enriched *Lactobacillus plantarum* causes more anti-carcinogenic effect on human colon cancer cells compared to non-enriched ones. *BioNanoScience*. 2023; 13: 1110-1115.
21. Shakibaie M, Khorramizadeh MR, Fara-marzi MA, Sabzevari O, Shahverdi AR. Biosynthesis and recovery of selenium nanoparticles and the effects on matrix metalloproteinase-2 expression. *Biotechnol Appl Biochem*. 2010; 56(1): 7-15.
22. Shield KD, Ferlay J, Jemal A, Sankara-narayanan R, Chaturvedi AK, Bray F, Soerjomataram I. The global incidence of lip, oral cavity, and pharyngeal cancers by subsite in 2012. *CA Cancer J Clin*. 2017; 67(1): 51-64.
23. Speight PM. Update on oral epithelial dysplasia and progression to cancer. *Head Neck Pathol*. 2007; 1(1): 61-66.

24. Jayaraj G, Ramani P, Sherlin HJ, Premkumar P, Anuja N. Inter-observer agreement in grading oral epithelial dysplasia – A systematic review. *J Oral Maxillofac Surg Med Pathol.* 2015; 27(1): 112-116.
25. Astekar M, Metgud R, Sharma A, Soni A. Hidden keys in stroma: Unlocking the tumor progression. *Oral Maxillofac Pathol.* 2013; 17(1): 82-88.
26. Alghezi DA, Aljawher R, Al-Musawi S. Increased CD73 expression is associated with poorly differentiated Gleason score and tumor size in prostate cancer. *J Adv Biotechnol Exp Ther.* 2023; 6(1): 161-171.
27. Sonkusre P, Cameotra SS. Biogenic selenium nanoparticles induce ROS-mediated necroptosis in PC-3 cancer cells through TNF activation. *J Nanobiotechnology.* 2017; 15(1): 43.
28. Xia Y, You P, Xu F, Liu J, Xing F. Novel functionalized selenium nanoparticles for enhanced anti-hepatocarcinoma activity *in vitro*. *Nanoscale Res Lett*. 2015; 10(1): 1051.
29. Patrón-Romero L, Luque-Morales PA, Loera-Castañeda V, Lares-Asseff I, Leal-Ávila MÁ, Alvelais-Palacios JA, Plasencia-López I, Almanza-Reyes H. Mitochondrial Dysfunction Induced by Zinc Oxide Nanoparticles. *Crystals.* 2022; 12(8): 1089.
30. Wang J, Liu N, Su Q, Lv Y, Yang C, Zhan H. Green synthesis of gold nanoparticles and study of their inhibitory effect on bulk cancer cells and cancer stem cells in breast carcinoma. *Nanomaterials (Basel).* 2022; 12(19): 3324.
31. Zeng D, Zhao J, Luk KH, Cheung ST, Wong KH, Chen T. Potentiation of *in vivo* anticancer efficacy of selenium nanoparticles by mushroom polysaccharides surface decoration. *J Agric Food Chem*. 2019; 67(10): 2865-2876.
32. Liao G, Tang J, Wang D, Zuo H, Zhang Q, Liu Y, Xion H. Selenium nanoparticles (SeNPs) have potent antitumor activity against prostate cancer cells through the upregulation of miR-16. *World J Surg Oncol*. 2020; 18(1): 81.
33. Varlamova EG. Molecular mechanisms of the therapeutic effect of selenium nanoparticles in hepatocellular carcinoma. *Cells.* 2024; 13(13): 1102.
34. Tian J, Wei X, Zhang W, Xu A. Effects of selenium nanoparticles combined with radiotherapy on lung cancer cells. *Front Bioeng Biotechnol*. 2020; 8: 598997.
35. Tang G, Zhen Y, Xie W, Wang Y, Chen F, Qin C, Yang H, Du Z, Shen Z, Zhang B, Wu Z, Tian D, Hu H. Preoperative hemoglobin-platelet ratio can significantly predict progression and mortality outcomes in patients with T1G3 bladder cancer undergoing transurethral resection of bladder tumor. *Oncotarget.* 2018; 9(26): 18627-18636.
36. Nori-Garavand R, Hormozi M, Narimani L, Beigi Boroujeni N, Rajabzadeh A, Zarei L, Beigi Boroujeni M, Beigi Boroujeni M. Effect of selenium on expression of apoptosis-related genes in cryomedia of mice ovary after vitrification. *Biomed Res Int*. 2020; 2020: 5389731.
37. Alkhudhayri AA, Wahab R, Siddiqui MA, Ahmad J. Selenium nanoparticles induce cytotoxicity and apoptosis in human breast cancer (MCF-7) and liver (HepG2) cell lines. *Nanosci Nanotechnol Lett*. 2020; 12: 324-330.
38. Assoian RK, Klein EA. Growth control by intracellular tension and extracellular stiffness. *Trends Cell Biol*. 2008; 18(7): 347-352.
39. Donnellan R, Chetty R. Cyclin D1 and human neoplasia. *Mol Pathol*. 1998; 51(1): 1-7.
40. Alao JP. The regulation of cyclin D1 degradation: roles in cancer development and the potential for therapeutic invention. *Mol Cancer.* 2007; 6: 24.
41. Wadhwani SA, Shedbalkar UU, Singh R, Chopade BA. Biogenic selenium nanoparticles: current status and future prospects. *Appl Microbiol Biotechnol*. 2016; 100(6): 2555-2566.
42. Hosnedlova B, Kepinska M, Skalickova S, Fernandez C, Ruttkay-Nedecky B, Peng Q, Baron M, Melcova M, Opatrilova R, Zidkova J, Bjørklund G, Sochor J, Kizek R. Nano-selenium and its nanomedicine applications: a critical review. *Int J Nanomedicine*. 2018; 13: 2107-2128.
43. Huang G, Liu Z, He L, Luk KH, Cheung ST, Wong KH, Chen T. Autophagy is an important action mode for functionalized selenium nanoparticles to exhibit anti-colorectal cancer activity. *Biomater Sci*. 2018; 6(9): 2508-2517.
44. Vekariya KK, Kaur J, Tikoo K. ERα signaling imparts chemotherapeutic selectivity to selenium nanoparticles in breast cancer. *Nanomedicine.* 2012; 8(7): 1125-1132.
45. Al-Muswie RT, Enayah SH, Ghaleb RA. Synergistic effects of Cassia fistula extract combination with cisplatin on the regulation of microRNA-145 and gene expression in colon cancer cell line SW480. *Med J Babylon.* 2023; 20(4): 670-680.